24th COBEM - 2017

24th ABCM International Congress of Mechanical Engineering
December 3-8, 2017, Curitiba, PR, Brazil

COBEM-2017-5900
SLAT NOISE: EXPERIMENTAL AND NUMERICAL EFFORTS AT USP-SÃO CARLOS

Daniel S. Souza
Universidade Federal de São João del Rei, Praça Frei Orlando, 170, São João del Rei
daniel.sampaio@ufsj.edu.br
Carlos C. Pagani Jr.
Universidade Estadual Paulista, Av. Profa. Isette Corrêa Fontão, 505, São João da Boa Vista
carlos.pagani@sjbv.unesp.br
Filipe R. do Amaral
Fernando H. T. Himeno
Universidade de São Paulo, Av. João Dagnone, 1100, São Carlos
framaral@gmail.com, fernando.himeno@gmail.com
Daniel Rodríguez
Pós-Graduação em Engenharia Mecânica (PGMEC),Universidade Federal Fluminense, Rua Passo da Pátria, 156, Niterói
danielrodriguez@id.uff.br
Marcello A. F. de Medeiros
Universidade de São Paulo, Av. João Dagnone, 1100, São Carlos
marcello@sc.usp.br

Abstract. *This paper summarizes the efforts and main achievements by the authors on the topic of slat noise. Wind tunnel experiments and numerical simulations with a Lattice-Boltzmann commercial code were performed in the studies and cross-correlation techniques were used to process the measured and simulated data. The effect on the noise signature of the Mach and Reynolds numbers, angle of attack, slat settings and excrescences on the slat cove wall were considered. Reliable data were generated and the results corroborated previous observations, revealed tendencies and contributed to elucidate aspects of dominant slat noise generation mechanisms.*

Keywords: *Slat noise, Acoustic Beamforming, Lattice-Boltzmann method, Proper Orthogonal Decomposition*

1. INTRODUCTION

Restrictions imposed by aviation authorities to airplane community noise are progressively more stringent. The introduction of ultra-high by-pass ratio turbofans in commercial aviation elevated the relative contribution of the airframe to the emission of external aeroacoustic noise, mainly in the landing phase. Together with the landing-gears and flap side edge, the slat constitutes one of the main airframe noise contributors, particularly in regional airplanes (Dobrzynski, 2010) as the ones predominantly produced by the Brazilian national industry.

Wind-tunnel experiments allowed the identification of the typical spectral distribution of the slat noise in low-Reynolds number models to be constituted of a hump around St=20, a broadband portion between St=0.1 and St=15 and a series of narrowband peaks superimposing the broadband component between $St = 1$ and 8, where St is the Strouhal number based on the free-stream velocity and the slat chord (Imamura *et al.*, 2009). Dobrzynski and Pott-Pollenske (2001) observed the slat noise power scales with the free-stream velocity based on a $5th$ power law. However, the better collapse of their data occurred based on a $4.5th$ power low, which suggests a combination of edge scatter ($5th$ power low) and monopole emission pattern ($4th$ power low) effects. Vortex shedding from the slat trailing edge is broadly accepted as the mechanism responsible for the high-frequency hump (Khorrami *et al.*, 2001, 2002; Choudhari *et al.*, 2002). The low- to mid-frequency noise portion is associated to perturbations in the slat cove free-shear layer in a general way and no incontestable evidence of a precise mechanism has been shown yet.

Several studies were dedicated to the effect of the slat configuration relative to the main element (deflection, gap, and overlap) and indicated the sensitiveness of the noise spectrum to these parameters (Pott-Pollenske *et al.*, 2003; Mendoza *et al.*, 2002; Emunds and Fischer, 2006; Takeda *et al.*, 2004). Nevertheless, these efforts were focused on the broadband and vortex shedding noise. On the other hand, the effects of installation devices received less attention, as the community has been concentrated in the identification of the fundamental mechanisms behind the slat noise generation.

This paper aims at summarizing the studies carried out by our group on the issue of slat generated noise under the

support of, or inspired by, the Silent Aircraft Project FAPESP/EMBRAER. Our experimental and numerical efforts have been oriented toward the description of the noise characteristics as well as to the analysis of the turbulent flow field in the slat region, with focus on the identification of the hydrodynamic events responsible for the generation of the narrowband peaks. The effects of the slat configuration and installation devices were studied at different Reynolds numbers and angles of attack at low Mach number regime both experimentally and numerically. A broad range of conditions were investigated by means of experiments in a closed section wind tunnel. The suitability of such facilities for the study of slat aeroacoustics were thoroughly investigated. Beamforming processing combined with deconvolution techniques was applied to the microphone measurements for the identification of noise sources in the slat region and the spectral distribution of slat noise emission. As the wind-tunnel experiments provided limited information on the turbulent flow field, LBM simulations were employed to investigate the possible mechanisms related to noise generation. The Proper Orthogonal Decomposition technique was used to identify the coherent structures interacting with the airfoil surface in the slat cove region.

2. CROSS VALIDATION OF EXPERIMENTAL AND SIMULATION METHODOLOGIES

The studies were conducted on high-lift configurations based on the MD30P30N airfoil geometry (Fig. 1). Its original setting is described in Tab. 1, where the lengths are relative to the airfoil stowed chord, c_{stowed}, which was 0.5 m both in the experiments and simulations.

The experiments were conducted in a closed section, closed circuit wind tunnel whose test section was 1.3 m high, 1.7 m wide and 3.0 m long, with free-stream velocities varying between 24 and 34 m/s. The two-dimensional airfoil model spanned the tunnel height and the application of suction reduced the wind-tunnel wall boundary layer three-dimensional effects (Pagani *et al.*, 2016). Static pressure on the model surface was measured by pressure tappings, distributed over the model chordwise and spanwise directions. A 62-microphone phased array (Fonseca, 2010) was employed for the acoustic measurements, which allowed the map of noise source distribution and determination of its respectively integrated noise spectra. The acoustic data were processed with in-house codes (Pagani *et al.*, 2016; Pagani Jr. *et al.*, 2017; Amaral *et al.*, 2017a) combining the Beamforming technique (Dougherty, 2002) and DAMAS deconvolution algorithm (Brooks and Humphreys, 2006).

Figure 1. Cross-section of the MD30P30N high-lift airfoil.

Table 1. Geometrical settings of the MD30P30N airfoil. Lengths relative to the stowed chord.

	gap	overlap	deflection (δ)	chord
slat	2.95%	-2.50%	30°	15%
flap	1.25%	0.25%	30°	30%

Simulations were carried out using the PowerFLOW (Fares, 2006) commercial code, which is based on the Lattice-Boltzmann method (Chen and Doolen, 1998). The turbulence structures of small scales were modeled by $k-\epsilon$ RNG turbulence model with law of the wall assumption for the volumes closest to no-slip walls. The computational domain was three-dimensional, the wind-tunnel walls above and below the airfoil was modeled as free-slip walls, and periodic condition was imposed in the spanwise direction.

Figure 2 shows the noise spectrum results provided by conventional beamforming technique and *DAMAS* deconvolution method for representative cases. The main difference between the results regards the multiple narrowband peak component. *DAMAS* reduces the magnitude of the peaks and level in the valleys between them, which provides more salient peaks. Figure 2(b) and (c) shows an example of the source noise maps obtained by the conventional beamforming technique and *DAMAS* deconvolution for *baseline* configuration, 3° angle of attack (AoA) and 4 kHz frequency. A 12 dB/Hz dynamic range was employed and the free stream flows from left to right. Although the spectral estimates do not vary substantially between conventional beamforming and *DAMAS*, the maps of the latter provide considerably better source representations.

Aeroacoustic measurements on high-lift models benefit from the well defined boundary conditions of closed-section wind tunnels, which reduce uncertainties on flow incidence and render the experimental conditions easier to become

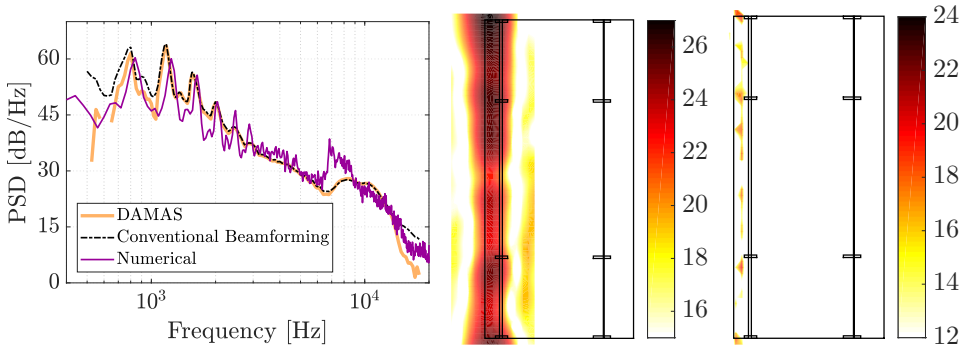

(a) Noise spectra (b) Conventional Beamforming, 4 kHz (c) *DAMAS*, 4 kHz

Figure 2. Comparison between Conventional Beamforming, *DAMAS* and numerical simulation for baseline configuration, 34m/s U_∞ and 3° AoA. Adapted from Amaral *et al.* (2017b).

numerically simulated. On the other hand, experiments with lifting bodies in hard-wall wind-tunnel test-sections suffer of drawbacks which jeopardize the accurate determination of both source signature and pressure level, as well as mirror sources associated with acoustic reverberation which may be mistaken by the real sources Fleury *et al.* (2015); Sijtsma and Holthusen (2003). Nevertheless, recent results show at least from low to moderate angles of attack, acoustic results obtained from measurements in closed-section wind-tunnels can reach a good agreement with free-field measurements Fleury *et al.* (2015) and numerical simulations (Pagani *et al.*, 2016).

The agreement level between the wind tunnel measurements and the Lattice-Boltzmann simulations used to analyze the turbulent flow field was discussed in Pagani *et al.* (2016) and is illustrated by the noise spectrum comparison in figure 2(a). Regarding the distribution of surface static pressure, the disagreements between the experiments and predictions were more pronounced in the flap suction side, where the simulations predicted a premature boundary layer separation. However, as shown in figure 2(a), low- to mid-frequency noise were well predicted, particularly the frequencies and amplitudes of the narrowband peaks. Therefore, the numerical simulations were deemed adequate for the investigation of the low frequency slat noise underlying mechanisms.

3. DOMINANT LOW FREQUENCY NOISE MECHANISM

The proper orthogonal decomposition was applied to three-dimensional slat cove flow data generated by lattice-Boltzmann simulations (Souza *et al.*, 2016) and transformed to the spanwised-time Fourier domain. Use of different correlation metrics in the POD computations allowed the rank of the educed coherent structures according to different objective criteria. In particular a metric based on the acoustic intensity in a plane bellow the airfoil allowed the rank of coherent structures according to their correlation to the noise emitted by the slat downwards.

The POD analyses based on the acoustic intensity indicated that the low frequency noise emitted by the slat is predominantly two-dimensional at the frequencies of the narrowband peaks and of deep between peaks. As an example, figure 3(a) shows a typical acoustic intensity based POD eigenvalue spectrum for the frequency of a narrowband peak. The shape of the dominant mode of this spectrum is shown in figures 3(b) and 3(c) and indicates that it is dominated by the spanwise mixing layer vortices.

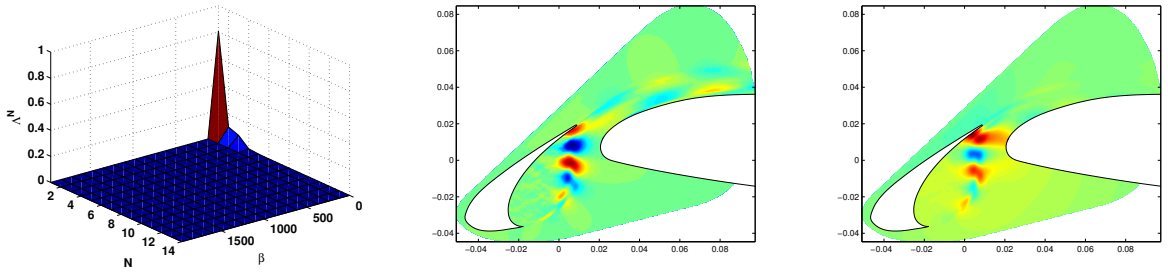

(a) (b) (c)

Figure 3. Acoustic intensity based POD results at the frequency of a narrowband peak (St=2.76). (a) Spectrum and real part of (b) X-Velocity and (c) pressure components. Reproduced from Souza *et al.* (2016).

The shape of the acoustic intensity POD modes suggested that the structures inside the slat cove most correlated to the acoustic emission are Kelvin-Helmholtz (K-H) vortices, and this was true for frequencies of the peaks and of deep between peaks (Souza, 2016). Therefore, the shapes of the dominant POD modes alone did not clarify the mechanism underlying the selection of the narrowband peaks. Olson *et al.* (2000) suggested that the slat cove works as an open cavity where a feedback cycle takes place similarly to the explained by Rossiter (1966) in the flow over open cavities. Theoretical formulas based on Rossiter's model had relative success in trying to predict the frequency of the narrowband peaks. However, they had either failed to predict the effect of angle of attack (Kolb *et al.*, 2007) or not tried (Deck and Laraufie, 2013; Terracol *et al.*, 2016).

Analyses by Souza *et al.* (2016) of the time evolution of dominant acoustic intensity based POD modes along the mixing layer path, $0<S<S_{max}$, and a straight line between the reattachment point and the cusp, $0<L<L_a$ (see figure 4(a)) further indicated the occurrence of the feedback loop as proposed by Terracol *et al.* (2016) for the slat geometry. Figures 4(b) and 4(c) show this time evolution along the loop path for a Strouhal number associated to a narrowband peak of the slat noise spectrum. The blue lines represent the hypothetical evolution of the fourth Rossiter-like loop and agrees very well with the actual evolution of the structures educed by the POD analysis. This spatio-temporal diagram evidenced that the mixing layer disturbances are mainly introduced by the pressure wave emitted as the K-H vortices developed in the own mixing layer interacts with the airfoil surface at the reattachment point region.

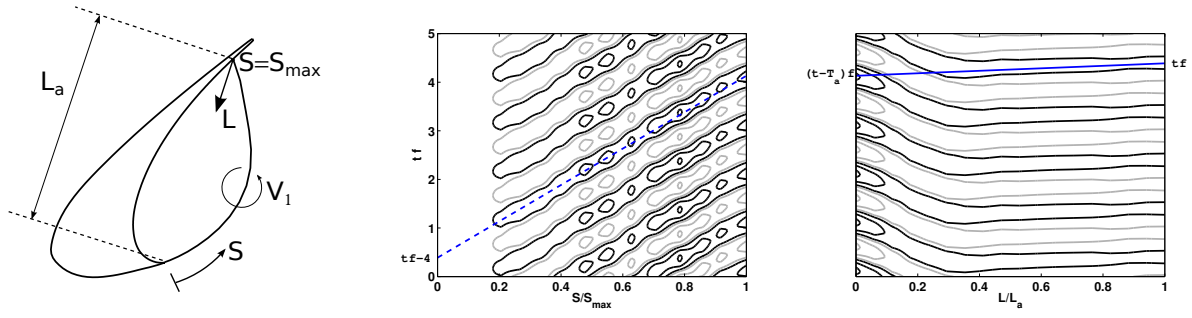

(a) (b) (c)

Figure 4. (a) Schematic representation of the disturbances in the feedback loop and time evolution of the disturbances captured by the dominant acoustic intensity based POD at the frequency of a narrowband peak (St=3.53): (b) along S and (c) along L. Reproduced from Souza *et al.* (2016).

4. EFFECT OF ANGLE OF ATTACK AND SLAT SETTING

The contour plots in Fig. 5 show the spectra variation for the baseline at 34 m/s U_∞ and a wide range of angles of attack, namely, from -6° to 18° (Amaral *et al.*, 2016, 2017a). The only salient spectral signatures are the high-frequency hump and the low-frequency narrowband peaks. Such peaks are more intense at 0°, sharply decay as the angle of attack is reduced and gradually decay as the angle of attack is increased. The frequency of the low-frequency narrowband peaks does not vary substantially in function of the angle of attack.

The noise spectra for angles of attack lower than -2° are broadband-like and their intensity levels are closer to those of the empty wind-tunnel. At 6°, the low-frequency narrowband peaks are reduced and the high-frequency broadband component becomes more relevant. For higher angles of attack, i.e., above 12°, the multiple narrowband peaks are suppressed and the slat noise approaches the empty wind-tunnel background noise. The high-frequency broadband hump generally reduces its intensity level in the frequency range investigated and may have moved to higher frequencies.

Measurements of different high-lift settings, considering variations of slat overlap, gap and deflection pointed to a large sensitiveness of the slat noise spectrum to these parameters (Pagani *et al.*, 2016). In particular, as shown in figure 6, among the range of parameters shown, the amplitude of the low frequency narrowband peaks decreases as the gap and/or overlap increase. However the effect of the gap on the narrowband peak emission power showed to be sensitive to the overlap setting. For instance, researches of the German Aerospace Center (DLR), as for example Pott-Pollenske *et al.* (2003); Ewert *et al.* (2010); Herr *et al.* (2015), identified an increase of the low frequency slat noise as the gap increased, at slightly positive overlaps, while the overlap of the cases represented in figure 6(a) was -1.6% of the stowed chord. As shown in figure 6(b), with a fixed gap of 2.95% of c_{stowed}, the narrowband peak frequencies reduced as the overlap increased, while the gap had no significant impact on the peak frequencies. The slat deflection at (gap;overlap)=(2.95%;-1.6%) affected mainly the high frequency hump (figure 6(c)). Comparison of the noise spectra and the chordwise mean static pressure distribution by Pagani *et al.* (2016) suggested a great influence of the main element suction peak on the emitted slat noise.

Among the different slat settings tested in the wind tunnel, two variations from the baseline MD30P30N were simu-

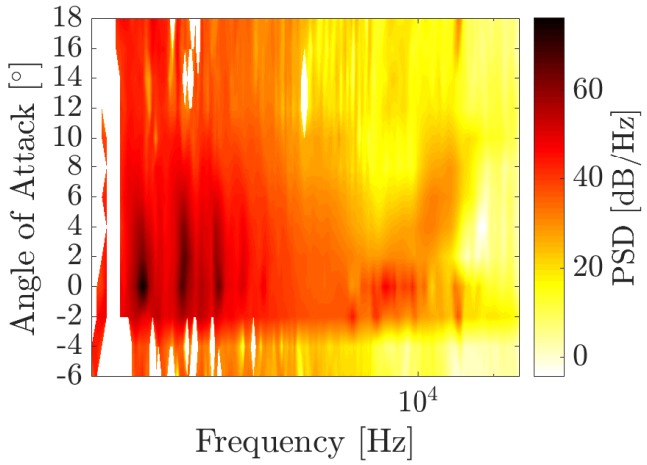

Figure 5. Power Spectral Density contour plots for baseline configuration at 34 m/s U_∞. Reproduced from Amaral *et al.* (2017a)

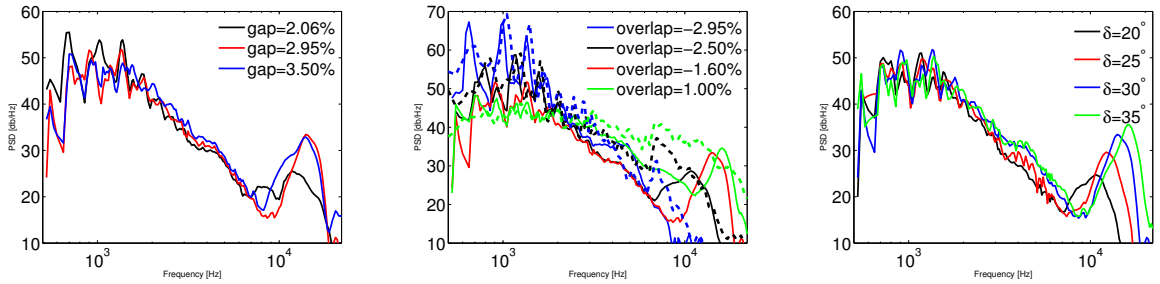

(a) (b) (c)

Figure 6. Effect of slat settings on the noise power spectral density. Effect of (a) gap, of (b) overlap (Dashed lines refer to numerical results) and of (c) deflection angle. Adapted from Pagani *et al.* (2016).

lated, one with overlap of -2.95% and other of 1.00% of the stowed chord (Souza, 2016). For these simulations, the slat gap and deflection were equal to the baseline. The agreement level between the numerical predictions and the measurements is illustrated in figure 6(b), where the dashed lines represent numerical results.

Figure 7(a) shows the time averaged streamlines representing the mean mixing layer path, revealing a large impact of both the angle of attack and the overlap on the size of the recirculating zone. As the AoA or the overlap increases, the size of the bubble reduces moving the reattachment point away from the slat trailing edge. The evolution of the turbulent kinetic energy along the mixing layer path is shown in figure 7(b) revealing that, among the simulated cases, the quietest one, with 1.00% overlap, had the most energetic mixing layer. The reason for this apparent inconsistency is still unclear, but the analyses made so far sustain two hypothesis. One is that the amplification effect of the slat trailing edge is weakened since its distance to the spanwise mixing layer vortices increases significantly for the 1.00% overlap configuration in comparison to the other simulated settings. Other hypothesis is that the dynamics of the smaller recirculation zone favors the amplification of three-dimensional structures, reducing the coherence of the mixing layer structures. This second possibility is sustained by computations of the spanwise coherence at the reattachment point, γ, shown in figure 7(c), γ being defined as

$$\gamma^2 = \frac{G^2_{z_1 z_2}(f, \Delta z)}{|G_{z_1 z_1}(f)||G_{z_2 z_2}(f)|}, \tag{1}$$

where $G_{z_1 z_2}(f, \Delta z)$ is the cross-spectral density between pressure signals at points z_1 and z_2 spaced Δz in the spanwise direction at frequency f and $G_{z_1 z_1}(f)$ is the power spectral density at point z_1. For the three slat settings simulated, POD analyses indicated that the spanwise mixing layer vortices were the structures most correlated to the noise emanating from the slat cove and revealed evidences of pressure feedback mechanism.

Either by changing the distance between the reattachment point and slat trailing edge or by the dynamics of the recirculating zone, the time-averaged mixing layer flow pattern seems to be of fundamental relevance to the amplitude of low frequency slat noise. Moreover, as discussed by Souza (2016), the mixing layer paths shown in figure 7(a) seemed

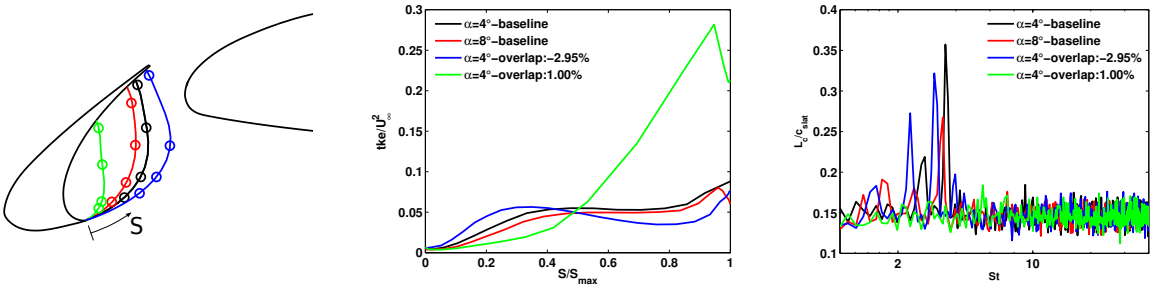

(a) (b) (c)

Figure 7. (a) Mixing layer path, (b) TKE along the mixing layer path and (c) spanwise coherence of pressure signals at the reattachment point. Reproduced from Souza (2016).

to be highly influenced by the upwash caused by the high speed flow over the main element leading edge. Therefore, the numerical results further evidence the influence of the main element suction peak on the slat noise, as identified by the experiments.

5. EFFECTS OF SEALING DEVICE

For the assessment of the cove wall bulb seal effect on the slat noise spectra, seals of different cross-sections, i.e., square, rectangular and circular edges, were tested (Amaral *et al.*, 2014, 2015). The seal position on the slat cove, d_{seal}, was defined by the distance between the seal leading edge end the slat trailing-edge, according to the schema in Fig. 8(c), which also applies to seals of squared and rectangular cross-sections. The squared and the rounded edge cross-section seals had 3 mm edges and 3 mm diameter, respectively, which corresponded to 4% of the slat chord, whereas the heights of the rectangular cross-section seals were 1 and 5 mm, corresponding to 1.3% and 6.7% of c_{slat}, respectively. The smaller rectangular seal was 0.3 mm high (0.4% of c_{slat}) and the wider seal was 6 mm wide (8% of c_{slat}). The slat cove seals spanned the entire slat model.

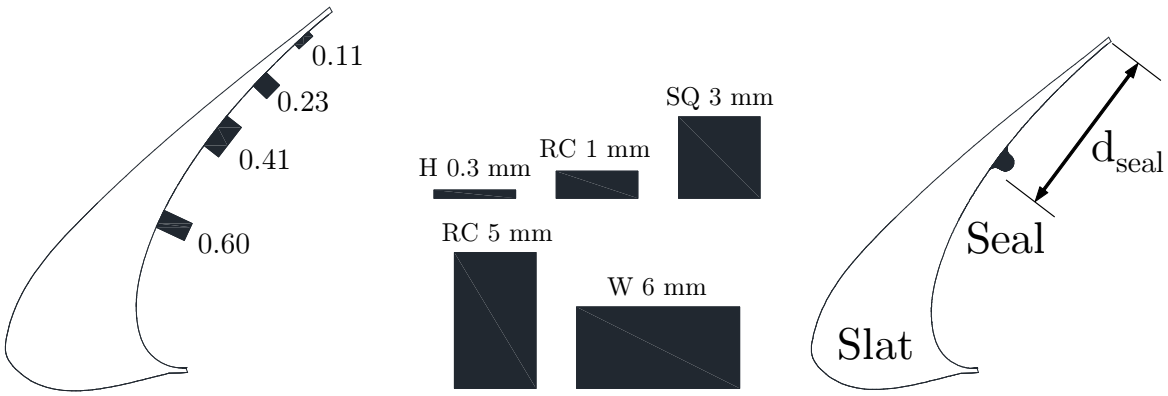

(a) d_{seal}/c_{slat}=0.11, 0.23, 0.41 and 0.60 (b) Seal cross-section tested (c) Distance d_{seal}

Figure 8. Seal configurations. Adapted from Amaral *et al.* (2017b).

The presence of a seal on the slat cove wall did not affect the static pressure distribution significantly (Amaral *et al.*, 2015). Figures 9a and 9b exhibits the effects of seal position and height respectively (thin lines refer to numerical results), and figure 9c compares different seal cross-sections on the slat noise spectra for 3° angle of attack and 34 m/s free-stream speed. The seal strongly impacted the slat noise spectrum and determined the dominant peak, i.e., the most intense one. The low-frequency narrowband peaks of the 1 mm height seal were similar to those of the baseline configuration, whereas the noise spectra of the 5 mm height seal were similar to those of the 3 mm height seal. At position 0.27, no seal had a very strong effect, whereas for position 0.41, i.e., the noisiest one, even the 1 mm height seal had a strong effect, similar to the 5 mm height seal. The high frequency hump slat spectra component was unaffected for any seal height - an exception was the slightly reduction in the spectral hump magnitude for seals of height equal to or higher than 3 mm. Mach and Strouhal noise spectra collapses were unaffected by the presence of a seal on the slat cove wall, for any of the positions tested, i.e., a good data collapse, similar to that obtained for the baseline configuration, was achieved for the $4.5 - th$ power of the Mach number and as function of the Strouhal number based on the free-stream speed and slat chord.

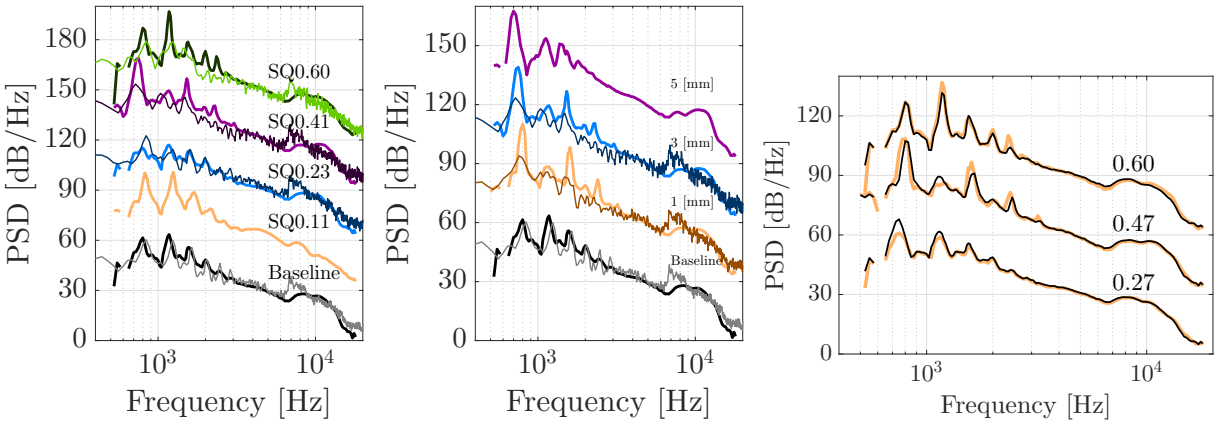

(a) (b) (c)

Figure 9. (a) Effect of seal position, (b) of seal height and (c) of seal cross-section shape (squared and rounded-edge). Adapted from Amaral *et al.* (2017b).

The far field numerical results captured the low-frequency narrowband peaks frequencies, although their magnitude was not well recovered for the sealed configurations when compared with the experiments, Fig. 9. For seal position d_{seal}/c_{slat}=0.23, for which the seal reduced the noise in the experiments, the cove seal represented a barrier that prevented the recirculation of the slat cove bubble turbulent structures. At other positions, the slat cove seal promoted a large boundary layer separation on the slat cove surface and produced a secondary bubble, Fig 10. Under these circumstances, the turbulence is more efficiently convected from the reattachment region directly to the slat cusp. In comparison with the baseline configuration, the generation of Kelvin-Helmholtz vortices in the mixing layer is enhanced, which may be associated with the acoustic noise increase observed experimentally.

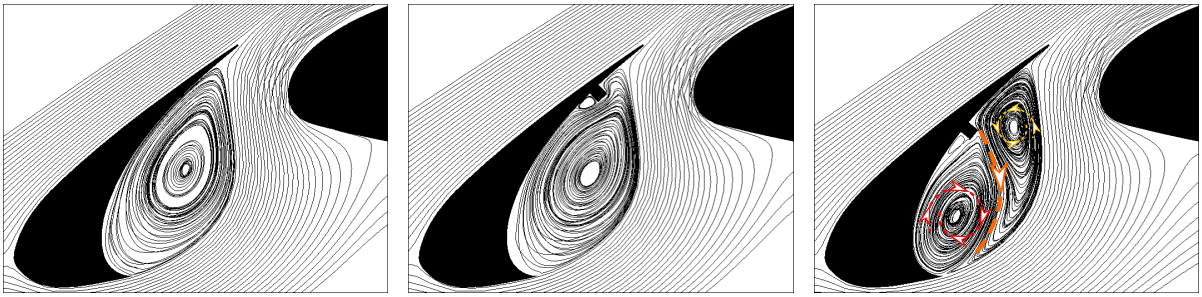

(a) Baseline (b) d_{seal}/c_{slat}=0.23 (c) d_{seal}/c_{slat}=0.41

Figure 10. Mean flow streamlines for baseline and sealed configurations for 3° AoA. Adapted from Amaral *et al.* (2017b).

Further LBM simulations were performed for the higher Reynolds number of 1.7 million (Bandle *et al.*, 2012; Souza *et al.*, 2015). These simulations intended to reproduce the conditions of NASA's Basic Aerodynamic Research Tunnel (BART) (Jenkins *et al.*, 2004) and considered free-slip condition for the slat surface outside the cove justified by the study by Simões *et al.* (2011). Similarly to the simulations at Re=1$\times$10^6, for the BART conditions, two flow regimes depending on seal position were identified, one with one big bubble and one with two counter rotating recirculating zones. However, contrary to the observations at 1 million Reynolds number, at the BART configuration, the two flow regimes resulted in an increase of low frequency slat noise, particularly the narrowband peaks, as shown in figure 11(a).

For Re=1.7$\times$10^6, the seal also seemed to work as a barrier to the small structures entrapped in the recirculating zone. Moreover, POD analysis based on the data of the center plane from the Re=1.7$\times$10^6 simulation, performed by Souza *et al.* (2015) and illustrated in figures 11(b) and 11(c), showed that the spanwise mixing layer vortices were significantly more organized for the case with seal and only one recirculation than for the clean slat, what may justify the increase of the low frequency narrowband peak acoustic power. Therefore, the opposite behavior observed in the the lower Reynolds number simulations is still unclear.

The aircraft certification procedures heavily penalize the occurrence of spectral tonnes and since the seal acts in particular on the tonnes, a seal could be effectively used for reducing the narrowband peaks noise level under operating conditions. Interestingly, the positions for which the seal produced higher and lower noise levels do not vary significantly in function of the angle of attack.

(a) (b) (c)

Figure 11. (a) Power Spectral Density of slat noise for Re=1.7×10^6 illustrating the effect of seal position (Reproduced from Bandle *et al.* (2012)); and X-velocity component real part of pressure based POD mode at the frequency of a narrowband peak for (b) the clean slat cove and (c) a configuration with a seal (Reproduced from Souza *et al.* (2015)).

6. FINAL REMARKS

The paper summarizes experimental and numerical work the authors developed in slat noise. It is presented at COBEM as it was supported for a long time by agencies in Brazil and in the State of São Paulo, as well as the Brazilian aeronautical industry. Above all, it was inspired and motivated by the needs of this national industry.

As is conveyed by the paper, at the start there was concern about the experimental procedures, among them the use of phased array techniques in relatively small close section wind tunnels and the beamforming codes developed in house. There was also concern about the numerical procedures, in particular the use of PowerFLOW. The agreement achieved between measured and simulated acoustic fields was considered remarkable at that time and gave confidence that both procedures were adequate for further studies.

The experiments were efficient for a parametric study, which included Mach number, angle of attack and slat settings. To the authors knowledge these are still the largest experimental data produced for slat noise emission. The experimental data established trends and regimes of noise emission. For instance, it was established that good slat aerodynamic performance is likely to be associated with high noise emission. Subsequently, numerical simulations were carried out for a limited number of selected cases. The experiments did not measured the flow field, so the sound generation mechanisms were investigated using the numerical results. Different data processing techniques were employed, the POD was the most powerful and eventually established more firmly the existence of the Rossiter like mechanism which had been previously proposed.

From a practical perspective, the installation of a slat requires other devices. Among those investigated during this effort, the bulb seal was the most interesting and had a surprisingly large impact in the scale of the model. Depending mostly on its position in the slat cove, it could strongly increase noise or reduce substantially the low frequency narrow band peaks which are heavily penalized in the certification procedures. Once more, the numerical results indicated which type of flow was associated with higher and lower noise emission.

It is important to remark that the study was carried out for a scaled model. It is argued that at the airplane scale the slat emission is different. This issue is currently been investigated by several aeronautical research agencies in the World. Nevertheless the use of scaled model remains as the dominant approach for studying slat noise.

7. ACKNOWLEDGEMENTS

The authors thank several engineers from Embraer led by Micael do Carmo. We also thank NDF at USP São Paulo for providing license for PowerFLOW code and Prof. F. M. Catalano and the technical staff of SAA-EESC for help with the pressure instrumentation of the model and its installation in the tunnel. D.S.S. and F.R.A. received funding from Coordination for the Improvement of Higher Education Personnel (CAPES/Brazil), grant #DS00011/07-0. C.C.P. received support from National Council for Scientific and Technological Development (CNPq/Brazil), grant #141755/2012-1. F.H.T.H. received support from Sao Paulo Research Foundation (FAPESP/Brazil), grant #2016/02970-5. M.A.F.M. received support from CNPq/Brazil, grants #304243/2013-2 and 304859/2016-8. M.A.F.M., D.S.S. and C.C.P. from FAPESP/Brazil in the context of the Brazilian Silent Aircraft Program, grant #2006/52568-7.

8. REFERENCES

Amaral, F., Himeno, F., Souza, D., Rico, J. and Medeiros, M., 2014. "Study of the effect of protrusions on the slat noise using beamforming techniques and lattice-boltzmann method". In *XXXV Iberian Latin American congress on computational methods in egineering*. Fortaleza, Brazil.

Amaral, F.R., Himeno, F.H.T., Pagani Jr, C.C. and Medeiros, M.A.F., 2016. "Experiments on slat noise from -6 to 18 degrees angles of attack". In *46th AIAA Fluid Dynamics Conference*. American Institute of Aeronautics and Astronautics. doi:10.2514/6.2016-3629. URL `http://arc.aiaa.org/doi/abs/10.2514/6.2016-3629`.

Amaral, F.R., Himeno, F.H.T., Pagani Jr., C.C. and Medeiros, M.A.F., 2017a. "Noise from the slat of md30p30n three-element airfoil at extreme angles of attack". *AIAA Journal*. Submitted.

Amaral, F.R., Himeno, F.H.T., Pagani Jr., C.C., Souza, D.S. and Medeiros, M.A.F., 2017b. "Effect of the bubble seal on the slat noise". *AIAA Journal*. Submitted.

Amaral, F.R.d., Souza, D.S., PaganiJr, C.d.C., Himeno, F.H.T. and Medeiros, M.A.F., 2015. "Experimental study of the effect of a small 2d excrescence placed on the slat cove surface of an airfoil on its acoustic noise". In *Proceedings of the 21st AIAA/CEAS Aeroacoustic Conference*. Dallas, USA.

Bandle, L., Souza, D., Simões, L. and Medeiros, M., 2012. "On the detrimental effect of excrescences on the slat noise". In *Proceedings of the 18th AIAA/CEAS Aeroacoustic Conference*. Colorado Springs, USA.

Brooks, T. and Humphreys, W., 2006. "A deconvolution apprach for the mapping of acoustic sources(DAMAS) determined from phased microphone arrays". *Journal of Sound and Vibration*, Vol. 294, No. 4-5, pp. 856–879.

Chen, S. and Doolen, G.D., 1998. "Lattice Boltzmann method for fluid flow". *Annual Review of Fluid Mechanics*, Vol. 30, pp. 329–364.

Choudhari, M., Lockard, D., Macaraeg, M., Singer, B., Streett, C., Neubert, G., Stoker, W., Underbrink, J., Berkman, M., Khorrami, M. and Sadowski, S., 2002. "Aeroacoustic experiments in the langley low-turbulence pressure tunnel". Technical report, NASA, Hampton, USA.

Deck, S. and Laraufie, R., 2013. "Numerical investigation of the flow dynamics past a three-element aerofoil". *Journal of Fluid Mechanics*, Vol. 732, pp. 401–444.

Dobrzynski, W., 2010. "Almost 40 years of airframe noise research:what did we achieve?" *Journal of Aircraft*, Vol. 47, No. 2, pp. 353–367.

Dobrzynski, W. and Pott-Pollenske, M., 2001. "Slat noise source studies for farfield noise prediction". In *Proceedings of the 7th AIAA/CEAS Aeroacoustics Conference*. Maastricht, Holanda.

Dougherty, R.P., 2002. *Beamforming In Acoustic Testing*, Springer Berlin Heidelberg, Berlin, Heidelberg, pp. 62–97.

Emunds, R. and Fischer, M., 2006. "Effect of slat settings (gap and overlap) on slat noise based on a test vortex injected upstream of the slat-hook". In *Proceedings of the 12th AIAA/CEAS Aeroacoustic Conference*. Cambridge, USA.

Ewert, R., Dierke, J., Pott-Pollenske, M., Appel, C., Emunds, R. and Sutcliffe, M., 2010. "CAA-RPM prediction and validation of slat setting influence on broadband high-lift noise generation". In *Proceedings of the 16th AIAA/CEAS Aeroacustics Conference*. Stockholm, Sweden.

Fares, E., 2006. "Unsteady flow simulation of the ahmed reference body using a lattice Boltzmann approach". *Computers and Fluid*, Vol. 35, pp. 940–950.

Fleury, V., Bulté, J., Davy, R., Manoha, E. and Pott-Pollenske, M., 2015. "2d high-lift airfoil noise measurements in an aerodynamic wind tunnel". In *21st AIAA/CEAS Aeroacoustics Conference*. p. 2206. doi:10.2514/6.2015-2206.

Fonseca, W., 2010. "A different approach to archimedean spiral equation in the development of a high frequency array". In *II SAE Brasil International Noise and Vibration Congress*. Florianópolis, Brasil.

Herr, M., Pott-Pollenske, M., Ewert, R., Boenke, D., Siebert, J., Delfs, J., Rudenko, A., Büscher, A., Friedel, H. and Mariotti, I., 2015. "Large-scale studies on slat noise reduction". In *Proceedings of the 21st AIAA/CEAS Aeroacoustics Conference*. Dallas, USA.

Imamura, T., Ura, H., Yokokawa, Y. and Yamamoto, K., 2009. "A far-field noise and near-field unsteadyness of a simplified high-lift-configuration model (slat)". In *Proceedings of the 15th AIAA/CEAS Aeroacoustics Conference*. Miami, USA.

Jenkins, L.N., Khorrami, M.R. and Choudhari, M.M., 2004. "Characterization of unsteady flow structures near leading-edge slat: part I. PIV measurements". In *Proceedings of the 10th AIAA/CEAS Aeroacoustics Conference*. Manchester, UK.

Khorrami, M.R., Singer, B. and Berkman, M., 2001. "Time-accurate simulations and acoustic analysis of slat free-shear-layer". In *Proceedings of the 7th AIAA/CEAS Aeroacoustics Conference*. Maastricht, Holanda.

Khorrami, M.R., Singer, B. and Lockard, D., 2002. "Time-accurate simulations and acoustic analysis of slat free-shear-layer: PART II". In *Proceedings of the 8th AIAA/CEAS Aeroacoustics Conference*. Breckenridge, USA.

Kolb, A., Faulhaber, P., Drobietz, R. and Grünewald, M., 2007. "Aeroacoustic wind tunnel measurements on a 2D high-lift configuration". In *Proceedings of the 13th AIAA/CEAS Aeroacoustics Conference*. Rome, Italy.

Mendoza, J., Brooks, T. and Humphreys, Jr., W., 2002. "An aeroacoustic study of a leading edge slat configuration". *International Journal of Aeroacoustics*, Vol. 1, No. 3, pp. 241–274.

Olson, S., Flint, O. and Nelson, R., 2000. "A preliminary investigation into slat noise production mechanisms in a high-lift configuration". In *Proceedings of the 18th AIAA Applied Aerodynamics Conference*. Denver, USA.

Pagani, Jr., C., Souza, D.S. and Medeiros, M.A.F., 2016. "Slat noise: Aeroacoustic beamforming in closed-section wind tunnel with numerical comparison". *AIAA Journal*, Vol. 54, No. 7, pp. 2100–2115.

Pagani Jr., C.C., Souza, D.S. and Medeiros, M.A.F., 2017. "Experimental investigation on the effect of slat geometrical configurations on aerodynamic noise". *Journal of Souzand and Vibration*, Vol. 394, pp. 256–279.

Pott-Pollenske, M., Alvarez-Gonzalez, J. and Dobrzynski, W., 2003. "Effect of slat gap/overlap on farfield radiated noise". In *Proceedings of 9th AIAA/CEAS Aeracoustics Conference*. Hilton Head, USA.

Rossiter, J.E., 1966. "Wind-tunnel experiments on the flow over rectangular cavities at subsonic and transonic speeds". Technical report, Aeronautical Research Council, London, UK.

Sijtsma, P. and Holthusen, H., 2003. "Corrections for mirror sources in phased array processing techniques". In *9th AIAA/CEAS Aeroacoustics Conference*. p. 3196. doi:10.2514/6.2003-3196.

Simões, L.G.C., Souza, D.S. and Medeiros, M.A.F., 2011. "On the small effect of boundary layer thicknesses on slat noise". In *Proceedings of the 17th AIAA/CEAS Aeroacoustics Conference*.

Souza, D.S., Rodríguez, D. and Medeiros, M.A.F., 2016. "Large scales structures and noise generation in leading edge slat high lift airfoils". In *Proceedings of 10th Spring School on Transition and Turbulence*. São José dos Campos, Brazil.

Souza, D.S., Rodríguez, D., Simões, L. and Medeiros, M.A.F., 2015. "Effect of an excrescence in the slat cove: Flow-field, acoustic radiation and coherent structures". *Aerospace Science and Technology*, Vol. 44, pp. 108–115.

Souza, D., 2016. *Estudo numérico de grandes estruturas turbulentas responsáveis pela geração de ruído no eslate*. Ph.D. thesis, Escola de Engenharia de São Carlos, Universidade de São Paulo.

Takeda, K., Zhang, X. and Nelson, P., 2004. "Computational aeroacoustic simulations of leading-edge slat flow". *Journal of Sound and Vibration*, Vol. 270, pp. 559–572.

Terracol, M., Manoha, E. and Lemoine, B., 2016. "Investigation of the unsteady flow and noise generation in a slat cove". *AIAA Journal*, Vol. 54, No. 2, pp. 469–489.

9. RESPONSIBILITY NOTICE

The authors are the only responsible for the printed material included in this paper.